Short-term nodal congestion price forecasting in a large-scale power market using ANN with genetic optimization training

Majid MOAZZAMI, Rahmat Allah HOOSHMAND∗
Department of Electrical Engineering, University of Isfahan, Isfahan-IRAN
e-mails: m_moazzami@eng.ui.ac.ir, hooshmand_r@eng.ui.ac.ir

Abstract

In a daily power market, price and load forecasting are the most important signals for the market participants. In this paper, an accurate feed-forward neural network model with a genetic optimization Levenberg-Marquardt back propagation training algorithm is employed for short-term nodal congestion price forecasting in different zones of a large-scale power market. The use of genetic algorithms for neural network training optimization has a remarkable effect on the accuracy of price forecasting in a large-scale power market. The necessary data for neural network training are obtained by solving optimal power flow equations that take into account all effective constraints at any hour of the day in a single month. The structure of the neural network has 2 input signals of active and reactive powers for every load busbar in every hour of the programming model. These 2 signals are always available. In this study, an IEEE 118-bus power system is used to test the proposed method authenticity. This system is divided into 3 zones, and a neural network with genetic algorithm training optimization is employed for every zone. Performance of the proposed method is compared with ARIMA and GARCH time series for the same data. The simulation results show that the proposed algorithm is robust, efficient, and accurate. Therefore, the algorithm produces better results than the ARIMA and GARCH time series for short-term nodal congestion price forecasting.

Key Words: Price forecasting, nodal congestion price, artificial neural network, genetic algorithm

1. Introduction

In many countries, power systems have changed from vertical and centralized systems into open power markets. As a result of this reconstruction, the price of electricity has attracted the attention of the present market activities. The nonstorability of electrical energy, generation and demand balance at any moment, power transfer control due to transmission congestion, and unawareness and impartiality of consumers to the power price in the short term all lead to price instability, creating unwelcome price spikes [1]. Load and price forecasting are important tools for market participants. Economic growth, weather conditions, fuel prices, previous load

∗Corresponding author: Department of Electrical Engineering, University of Isfahan, Isfahan-IRAN

data, and the historical record of electricity prices in the power system, as well as power reduction, are the parameters affecting the price of electricity. Furthermore, electricity prices vary according to the hour of the day, the day of the week, the season, and holidays. Therefore, a good price forecasting system must be able to forecast the price of electricity with acceptable errors, regarding all available uncertainties in the power system. Furthermore, the load value is the most important price-driven variable for short-term forecasting.

Price forecasting models are typically divided into conventional and modern methods. The conventional price forecasting models include time series models and regression analysis [2]. The use of artificial intelligence methods for price forecasting has become very common in recent years. Out of these methods, the use of neural networks is a simple and strong tool for price forecasting. Neural networks are able to determine the relationship between the input and output of every intricate problem using data and the historical record. Furthermore, time series can represent the relationship between electricity price and the nonlinear parameters of power demand, weather conditions, and generation amount. Autoregressive integrated moving average (ARIMA) [3,4], seasonal ARIMA (SARIMA) [5], and generalized autoregressive conditional heteroskedasticity (GARCH) [6] are the most general time series for price forecasting. In [5], a price forecasting mechanism using the combined SARIMA model and a discrete non-time-homogeneous Markov process was proposed. It was shown that out of the statistical models, the dynamic regression and the transfer function models had better results than the ARIMA model for the Californian and Spanish power markets [7]. With an improvement in price forecasting methods through the use of a time series, the GARCH model has been used in these markets [7]. A hybrid of the artificial neural network (ANN) and ARIMA models for price forecasting in the Australian power market was introduced in [8]. The results obtained from that study show that using the hybrid model by itself is more accurate than either ANNs or ARIMA alone.

In [9], the k-weighted nearest neighbors with dynamic regression were used for price forecasting. In [10], a stochastic game theory model and a reinforcement learning (RL)-based solution framework were developed for price forecasting in a day-ahead power market. The RL-based approach was utilized to obtain an approximate solution for the game theoretic model. These solutions provide effective bidding strategies for the day-ahead market participants.

ANNs have been employed for price forecasting for practical power systems in different countries. In [11-13], a neural network was utilized for market clearing price (MCP) estimation and effective uncertainty analysis of price forecasting. ANNs were successful price forecasting tools in California [7], the UK power pool [14], the PJM [15], and Australian power markets [16]. In [17], it was shown that using a feed-forward neural network is more accurate and efficient compared to time series methods such as ARMA, GARCH, the adaptive neuro-fuzzy inference system (ANFIS), and recurrent neural networks. In [18], 2 ANNs were proposed for forecasting an hourly weighted average price and an hourly minimum accepted price in Iran's electricity market as a pay-as-bid market. In addition, fuzzy methods and their combinations with neural networks [1], the ANFIS method [19], support vector machines [20], combinations of neural networks and extended Kalman filters [15], ANNs and rough set theory [21], and ANNs and committee machines [11] are other tools proposed for price forecasting. The forecasting accuracy and computational complexity of most of these techniques were simulated and compared in [22].

This paper provides a feed-forward neural network with genetic algorithm (GA) training optimization for a short-term nodal congestion price (NCP), forecasting in different zones of an electricity market. The data required for the neural network database were obtained by solving optimal power flow (OPF) equations for the system load variations for each hour of the day in 1 month. This model is nonlinear, smooth, large-scale

programming. The data provided by the proposed method regarding the formation of various congestion zones and the severity of congestion within a zone would alert the independent system operator (ISO) to balance the system by applying an uplift to the MCPs within that zone. In this structure, the neural system has 2 signals of active and reactive powers of busbar loads in each hour of the programming model. These 2 signals are always available in the power system. The IEEE 118-bus test system is used for the proposed method's authenticity testing. The test system is divided into 3 zones and a neural network with GA training optimization is employed for every zone. The ARIMA and GARCH time series are used for comparing the results of the proposed method for the same data. The results show the ability of the proposed method for NCP forecasting in a large-scale power market with a lower and more acceptable error than the other 2 time series models.

2. Optimal power flow problem formulation

Contrary to the load curve, the price curve is a nonhomogeneous curve and its variations show little cyclic property. Although the price of electricity is very volatile, it is not regarded as random. Hence, it is possible to identify certain patterns and rules pertaining to market volatility. Using historical price data is a suitable way to forecast price spikes and the probability of their occurrence. Load and generation balance at any moment for a power system is the main reason for price volatility. Other reasons for price volatility include fuel cost volatility, time factors, weather conditions, different consumer classes, load uncertainty, fluctuations in hydroelectricity production, generation uncertainty, transmission congestion, behavior of market participants based on anticipated price, market manipulation, and special events such as the Olympic Games or various national ceremonies that increase power system demand [23].

In simulation processes regarding operation constraints of a power system, the OPF problem will be solved. Using a large amount of input data, a simulation can yield an appropriate estimation of the price curve. A simulation must contain an elaborate power system model and a procedure for a pricing system. Based on this mathematical model and the process mentioned above, price forecasting is accomplished.

For electricity price forecasting, some information, such as transmission system model, unit commitment programming, and distribution of safe and secure load transmissions, and the simulation ability of a large-scale power system are important. The optimization problem is described by Eq. (1).

$$
\begin{aligned}
&\min \sum_i \left(f_i \left(P_{gi} \right) \right) \\
&s.t. \\
&P_k = \sum_{i \in I_k} \left(P_{gi\circ} + P_{gi} \right) - \sum_{j \in J_k} \left(P_{L\circ j} + P_{Dj} \right) \\
&Q_k = \sum_{i \in I_k} \left(Q_{gi} \right) - \sum_{j \in J_k} \left(Q_{L\circ j} + Q_{Dj} \right) \\
&R_{r\ AGC} \left(g_i \right) = K, \forall i \in I \\
&R_r Q \left(g_i \right) = T, \forall i \in I \\
&P_{g\min i} \leq P_{gi} \leq P_{g\max i}, \forall i \in I \\
&Q_{g\min i} \leq Q_{gi} \leq Q_{g\max i}, \forall i \in I \\
&P_{D\min j} \leq P_{Dj} \leq P_{D\max j}, \forall j \in J \\
&V_{\min k} \leq V_k \leq V_{\max k}, \forall k \in B \\
&\left| P_{mk} \left(\theta, V \right) \right| \leq P_{mk\max}, \forall \left(mk \right) \in N \\
&\left| P_{km} \left(\theta, V \right) \right| \leq P_{km\max}, \forall \left(km \right) \in N \\
&I_{mk} \left(\theta, V \right) \leq I_{mk\max}, \forall \left(mk \right) \in N \\
&I_{km} \left(\theta, V \right) \leq I_{km\max}, \forall \left(km \right) \in N \\
&R_{g\min i} \leq R_{gi} \leq R_{g\max i}, \forall i \in I
\end{aligned}
\tag{1}
$$

Here, f_i is the active power generation cost of unit i and is simulated using the following quadratic equation:

$$f_i = C_\circ + C_1 P_{gi} + C_2 P_{gi}^2. \tag{2}$$

As has been pointed out, this optimization problem is large-scale, smooth, nonlinear programming. By solving this problem and using the Karush-Kuhn-Tucker theory, the lagrangian multipliers of the problem are obtained. The obtained equality lagrangian multipliers and the corresponding lagrangian function determine the shadow price of electricity required to satisfy system inequality constraints and maintain system security, or the NCP. In this formulation, transmission line current flow and real power transmission capacity are taken as system security parameters. By estimating the amounts of NCP in a reconstructed power market, congestion management of the power system can be achieved. The amount of NCP in a system not only shows the presence of congestion but also implies the severity of congestion in that system [13]. MATLAB software is employed for solving OPF equations.

3. The proposed algorithm for NCP estimation

The price of electricity in different points of the market depends on the physical characteristic of the power system and the operation conditions. A large volume of information and the presence of price spikes require a powerful tool for the identification of dominant rules for these data. Due to the unique ability of ANNs to recognize patterns, they can be efficient tools in price forecasting and were employed in this study. ANN input selection has a salient effect on the training accuracy and the ANN response. The process of database information calculation, ANN input selection, and the proposed algorithm employed in this study are described in the following paragraph.

3.1. Reasons for the selection of ANNs for price forecasting

Today, one of the most popular intelligence methods for load and price forecasting is the ANN. ANNs have more advantages than other price forecasting methods. The training ability and input-output relation learning, as well as the discovery of load and price from historical data without a need for an appropriate model, are the most important features of ANNs. Their easy implementation, suitable operation, obvious modeling, considerably high speed, desirable operation in different seasons of the year, and proper operation under different loading conditions are benefits of ANNs. The high speeds associated with ANNs allow for price forecasting with all effective constraints possible in a spot market. Basically, the impact of the transmission line capacity and the outage of the lines and generation units are homogeneous for the price of electricity. In other words, if we had enough historical data, we could determine the relationships between these parameters and the electricity price using an ANN. The impacts of load and price-suggested patterns on the actual electricity price are nonhomogeneous and the determination of these relationships requires OPF equations. The formulation method used in this study for the calculation of the NCP amount in the spot market was based on the pool market pattern. Under this condition, the NCP amounts are based on power price constraints. These amounts are paid by consumers and cashed by companies. OPF problem formulation uses one slack bus.

3.2. Input selection

The NCP amounts are very variable compared to the conditions of power system operation. Basically, the NCP amounts depend on the power system loading scenario. With this in mind, active and reactive powers of busbar loads are considered as the ANN input for NCP estimation.

3.3. Forecasting algorithm for nodal prices

The NCP algorithm estimation by an ANN is summarized as follows:

 1- Creating an hourly loading scenario for the system under study.

 2- Performing the OPF problem for the calculation of NCPs in all of the nodes for each loading scenario.

 3- Creating a separate ANN for every congestion zone and training respective ANNs for each zone.

 4- Testing ANNs for different load patterns not considered in the ANN database.

A flowchart depicting these stages is shown in Figure 1. Creation of power system loading scenarios in some works is random [13]. These scenarios may be different from the actual amounts of power system operation. It is important to emphasize that the amounts of NCPs are basically dependent on the power system loading scenario.
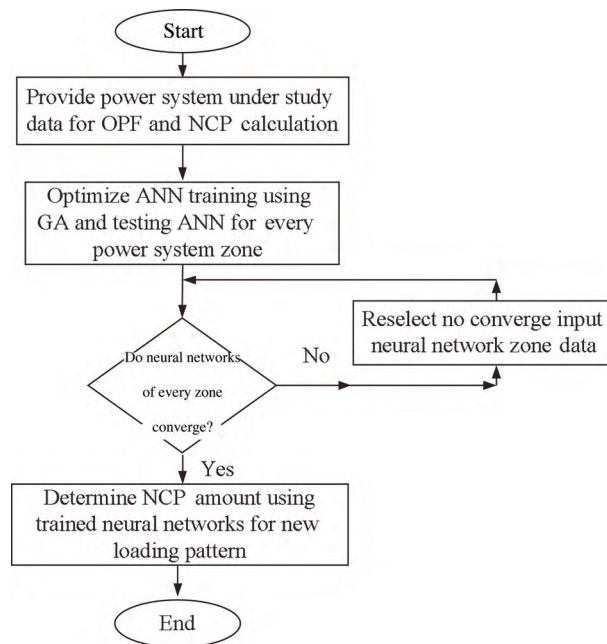

Figure 1. Proposed method flowchart for NCP estimation.

4. ANN structure with GA training optimization

The Levenberg-Marquardt training algorithm is faster faster than other ANN training methods. For the large amounts of data in this study, the Levenberg-Marquardt backpropagation (LMBP) algorithm was used to train the ANN ternary zones of the power system. In order to obtain the least amount of training error, the GA was used for the optimization of the input selections, steps sizes, momentum values, and the number of required processing elements in the hidden layers. Mean square error (MSE), root mean square error (RMSE), mean absolute error (MAE), and minimum and maximum of absolute error criteria were used for the performance analysis of the trained ANN.

4.1. ANN training algorithm using LMBP

In the LMBP algorithm, the data spread from the input layer to the hidden layers and then reach the final output layer. The error signals in the output layer spread to the hidden layers and the input layers. The sum-of-squares signals are then minimized by adjusting the synapse weight coefficients and are biased in all layers during the training process.

For a multilayer neural network, the input $v^{k+1}(i)$ and the output $y^{k+1}(i)$ from the ith neuron and in the $(k+1)$th layer are described by Eqs. (3) and (4), respectively.

$$v^{k+1}(i) = \sum_{j=1}^{s_k} w^{k+1}(i,j)y^k(j) + b^{k+1}(i) \tag{3}$$

$$y^{k+1}(i) = \phi^{k+1}(v^{k+1)}(i)) \tag{4}$$

Here, s_k is the number of outputs in the kth layer, and $w^{k+1}(i,j)$, $b^{k+1}(i)$, and ϕ^{k+1} are the synapse weight coefficients, bias function, and neuron excitation function of the ith neuron in the $(k+1)$th layer, respectively. For a k-layer neural network, the system matrix equations are as follows:

$$\bar{y}^{\circ} = \bar{p}, \tag{5}$$

$$\bar{y}^{k+1}(i) = \bar{\phi}^{k+1}(w^{k+1}\bar{y}^k + \bar{b}^{k+1})k = (0,1,\ldots k-1). \tag{6}$$

The input signals $\bar{p}$ with z variables are described as $[p(1), p(2), ..., p(Z)]^T$. Input-output $\{(\bar{p}_1, \bar{q}_1), (\bar{p}_2, \bar{q}_2), ...,$ $(\bar{p}_R, \bar{q}_R)\}$ vector couples are employed for training the ANN, and these pairs are assigned by parameter R. By depicting the sum-of-squares error as the performance index, the ANN error is obtained from the following error function:

$$E = \frac{1}{2}\sum_{r=1}^{R}(\bar{q}_r - \bar{y}_r^k)^T(\bar{q}_r - \bar{y}_r^k) = \frac{1}{2}\sum_{r=1}^{R}(\bar{e}_r)^T\bar{e}_r, \tag{7}$$

where $\bar{e}_r = \bar{q}_r - \bar{y}_r^k$ is the output error and $\bar{y}_r^k$ is the ultimate output of the rth input.

The squares error function, $E(\bar{x})$, is employed as the objective function, as follows:

$$E(\bar{x}) = \frac{\sum_{i=1}^{N} e_i^2(x)}{N}. \tag{8}$$

To minimize this objective function, Newton's method, based on the following equation, is employed:

$$\Delta\bar{x} = -\left[\nabla^2 E(\bar{x})\right]^{-1}\nabla E(\bar{x}). \tag{9}$$

Here, $\nabla E(\bar{x}) = J^T(\bar{x}) \cdot \bar{e}(\bar{x})$ and $\nabla^2 E(\bar{x}) = J^T(\bar{x}) \cdot J(\bar{x}) + S(\bar{x})$, where $J(\bar{x})$ is a Jacobian matrix and $S(\bar{x}) = \sum_{i=1}^{N} \bar{e}_i(\bar{x})\nabla^2\bar{e}_i(\bar{x})$ [24].

In this method, Eq. (9) is used to update Eq. (8). It is assumed that $S(\bar{x}) = 0$. Therefore,

$$\Delta(\bar{x}) = -\left[J^T(\bar{x}) \cdot J(\bar{x})\right]^{-1}J^T(\bar{x}) \cdot \bar{e}(\bar{x}). \tag{10}$$

The Levenberg-Marquardt algorithm modifies Newton's method by the following equation:

$$\Delta(\bar{x}) = -\left[J^T(\bar{x}) \cdot J(\bar{x}) + \mu \cdot I\right]^{-1} J^T(\bar{x}) \cdot \bar{e}(\bar{x}), \tag{11}$$

where the μ parameter is updated according to the performance index change in each iteration of the training process. In this equation, I is the identity matrix. It can be demonstrated that the performance index in Eq. (7) is equal to Eq. (8). For the LMBP algorithm, the R input-output vector couples are fed into the network. Outputs and errors are then calculated with Eqs. (5), (6), and (8). In the next stage, the Jacobian matrix and increasing changes of $\Delta\bar{x}$ are obtained from Eq. (11). Ultimately, the performance index is calculated again by replacing $\bar{x}$ with $\bar{x} + \Delta x$ to solve for $E(\bar{x})$. When the performance index is less than a specific error value, the ANN training process will be finished; in other words, the correction of the μ parameter is done for this iteration of the ANN training process.

4.2.   Genetic training procedure

In this study, the neural network training was performed based on a GA. This structure was used for the genetic optimization of the neural network and selection of the inputs, the size of the steps, momentum values, and the number of required processing elements in the hidden layers. The goal of optimization is to find the best adjustment for the parameters so that the training error is minimized. If cross-validation is used during the training process, the goal will be to minimize its error. Otherwise, the goal will be to minimize the training error. The best weights and parameter settings are selected for the ANN during training. To perform genetic training, an initial population of networks is first randomly created, each having a different set of parameters. Each of these networks is then trained and evaluated to determine its fitness based on the minimum error that it achieved. The characteristics of the best networks are then combined and mutated to create a new population of networks. The existing neural networks in this population are again evaluated and the best networks are selected, resulting in the next generation. This process is repeated until the maximum population or the maximum evaluation time is attained. Finally, the best ANN specifications are specified and used. This process leads to better ANN training, especially in the study at hand, with a large information database. Neuro-Solutions software was employed for the ANN training.

4.3.   Evaluation and testing criteria of the ANN

For the investigation of the ANN operation for price forecasting, the MSE, RMSE, and MAE were calculated for the tested items [21]. The equations representing the errors are expressed below.

$$MSE = \frac{\sum_{j=1}^{Ji} (P_{Aj} - P_{Fj})^2}{Ji} \tag{12}$$

$$RMSE = \sqrt{\frac{\sum_{j=1}^{Ji} (P_{Aj} - P_{Fj})^2}{Ji}} \tag{13}$$

$$MAE = \frac{\sum_{j=1}^{Ji} (P_{Aj} - P_{Fj})}{Ji} \tag{14}$$

5.   Simulation results

5.1.   The power system under study

In this study, the IEEE 118-bus standard power system was selected as the testing system. This system has 54 generators, 186 transmission lines, 14 capacitors, and 9 tap changer transformers. Full data for this system are available in [25]. The single-line diagram and its ternary zones are shown in Figure 2. With regard to seasonal variations, the peak load occurs at 2100 hours and its value reaches 7309 MW [26].
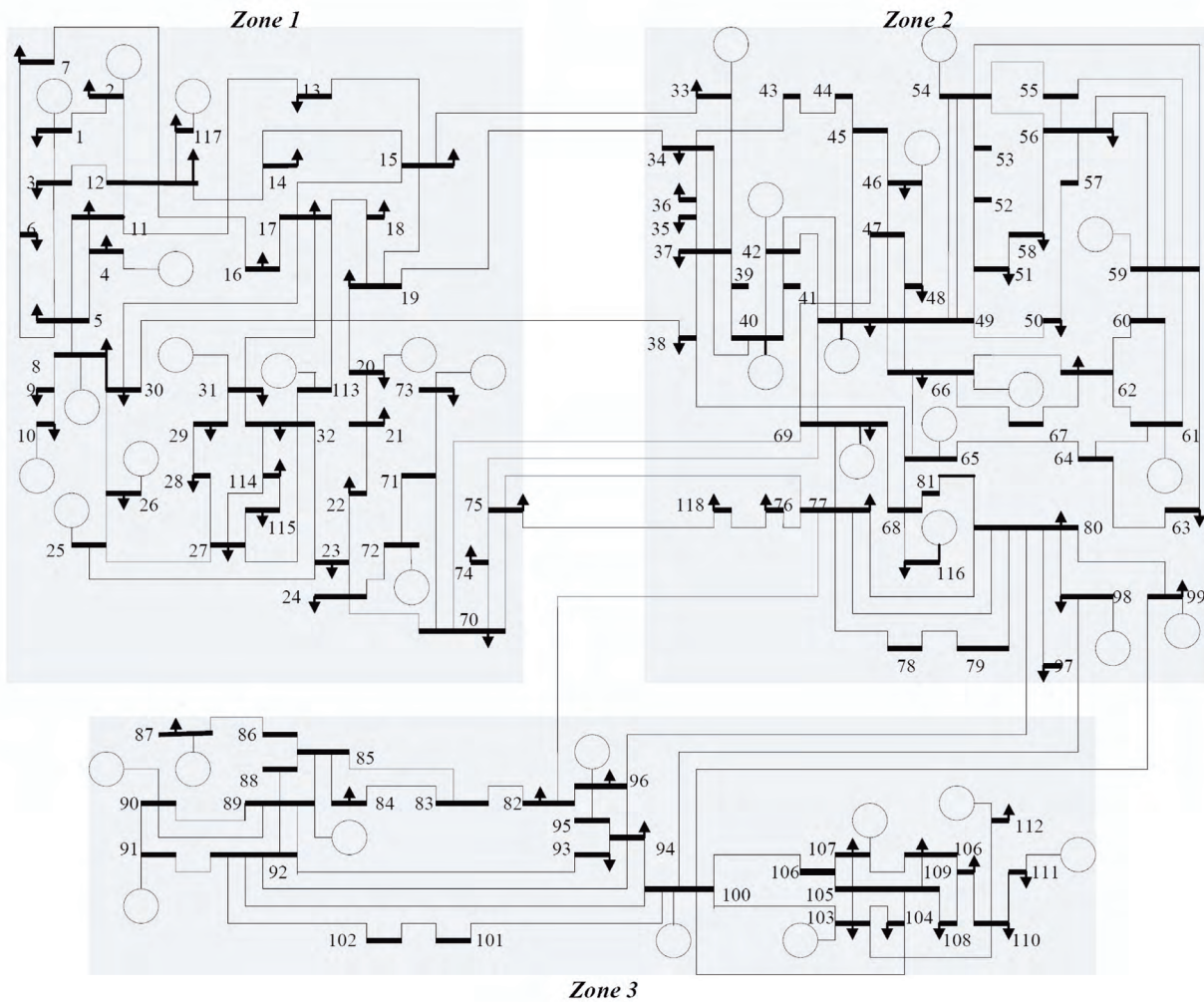

Figure 2. Single line of IEEE 118-bus test system and zone configuration.

Necessary database information for neural network training is obtained by solving optimal power flow equations for each hour of the day. For example, the base hourly loading scenario for day 1 is shown in Table 1. This process was performed for 1 month's worth of daily loading, considering daily load curve variation. This network was divided into 3 zones, with 22,611 data-sets in the first, 24,969 in the second, and 16,172 in the third, obtained for use in the ANN database. These values do not include data for days 10, 19, and 25, which were selected for ANN testing.

Table 1. Base hourly loading scenario for an IEEE 118-bus test system.

Hour	Real load (MW)	Reactive load (MVAR)	Hour	Real load (MW)	Reactive load (MVAR)
0100	4200	1623.47	1300	4800	1855.39
0200	3960	1530.70	1400	4560	1762.62
0300	3480	1345.16	1500	5280	2040.93
0400	2400	927.70	1600	5400	2087.31
0500	3000	1159.62	1700	5100	1971.35
0600	3600	1391.54	1800	5340	2064.12
0700	4200	1623.47	1900	5640	2180.08
0800	4680	1809.01	2000	5880	2272.85
0900	4920	1901.78	2100	6000	2319.24
1000	5280	2040.93	2200	5400	2087.31
1100	5340	2064.12	2300	5220	2017.74
1200	5040	1948.16	2400	4920	1901.78

5.2. ANN specification with GA training optimization

To obtain suitable ANN training, an ANN was considered for each zone. For the purpose of achieving appropriate behavior in price forecasting, many neural networks were trained. The best specifications and the resulting neural network parameters for the 3 zones are presented in Table 2. The conditions used for GA training of the ANNs are presented in Table 3.

Table 2. Specifications and neural network parameters for each zone.

ANN parameter	Zone 1	Zone 2	Zone 3
No. of input neurons	2	2	2
No. of output neurons	1	1	1
No. of hidden layers	2	2	1
No. of hidden layer neurons	1-(5), 2-(4)	1-(7), 2-(6)	20
Using neural network model	Feed-forward	Feed-forward	Feed-forward
Training network algorithm	LMBP	LMBP	LMBP
Transfer function midlayer neurons	Hyperbolic tangent	Hyperbolic tangent	Hyperbolic tangent
Transfer function output layer neurons	Hyperbolic tangent	Hyperbolic tangent	Hyperbolic tangent
Maximum of epoch	5000	500	1000
Error threshold	0.001	0.001	0.001
Weight update method	Batch	Batch	Batch

Table 3. GA training parameters of ANN used in each zone.

Genetic training parameters	Zone 1	Zone 2	Zone 3
Number of epochs	5000	500	1000
Population size	20	20	20
Maximum generation	25	25	25
Operator selection	Roulette	Roulette	Roulette
Crossover	Heuristic	Heuristic	Heuristic
Crossover probability	0.7	0.6	0.6
Mutation	Uniform	Gaussian	Gaussian
Mutation probability	0.03	0.03	0.03

The variation of 1 MWh of energy in terms of US$/MWh found in the nodes of zone 1 of the power system in the database used in the neural network training is shown in Figure 3a. In Figure 3b, the manners of the active and reactive power variations of zone 1 loads are shown. Figure 3c shows variations of the active power price in terms of $/MWh for zone 1 loads on the basis of nodal active power variations. The mentioned variations for zone 1 are similarly shown for zones 2 and 3 in Figures 4a-4c and 5a-5c, respectively.

Table 4. Minimum and final values of ANN genetic training.

Zone No.	Optimization summary	Best fitness	Average fitness
	Epochs	17	23
Zone 1	Min. MSE	0.014038224	0.014750256
	Final MSE	0.014038224	0.019557543
	Epochs	19	24
Zone 2	Min. MSE	0.012840169	0.013637662
	Final MSE	0.012840169	0.016617935
	Epochs	2	22
Zone 3	Min. MSE	0.009023999	0.009023999
	Final MSE	0.009023999	0.009192817
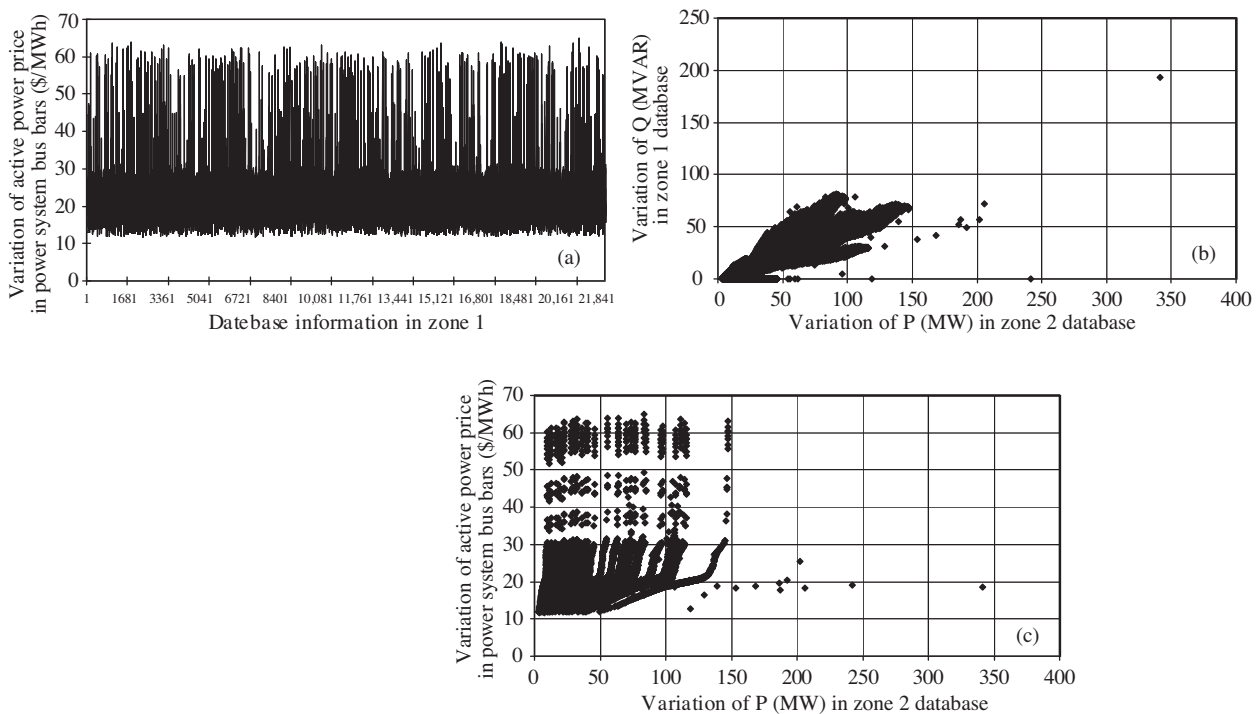
Figure 3. Zone 1 ANN database information: a) variation of 1 MWh of energy in terms of $/MWh, b) active and reactive power variations of loads, c) active power price variations in terms of $/MWh on the basis of active power variations.

In Table 4, the minimum and the final values of ANN genetic training errors in each of the 3 zones are provided. The neural network standard function curves, which show the best and average MSE fitness in terms of the generations, are presented in Figures 6a and 6b, respectively.
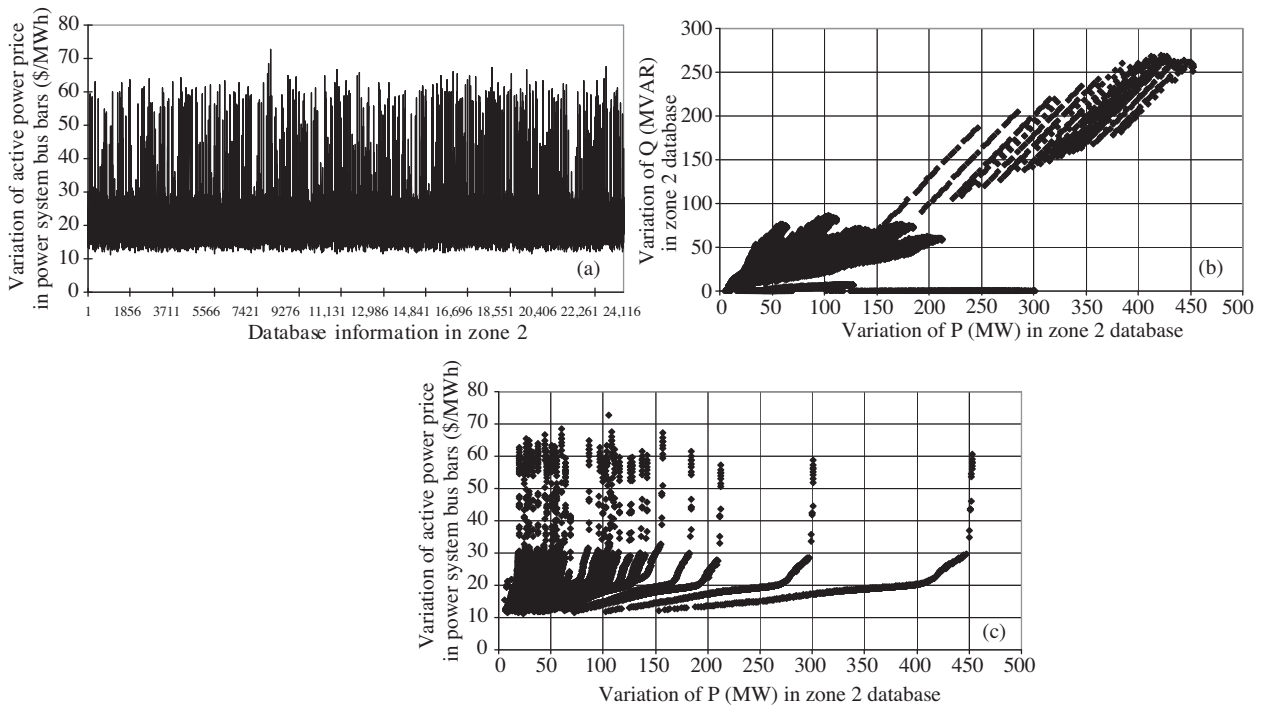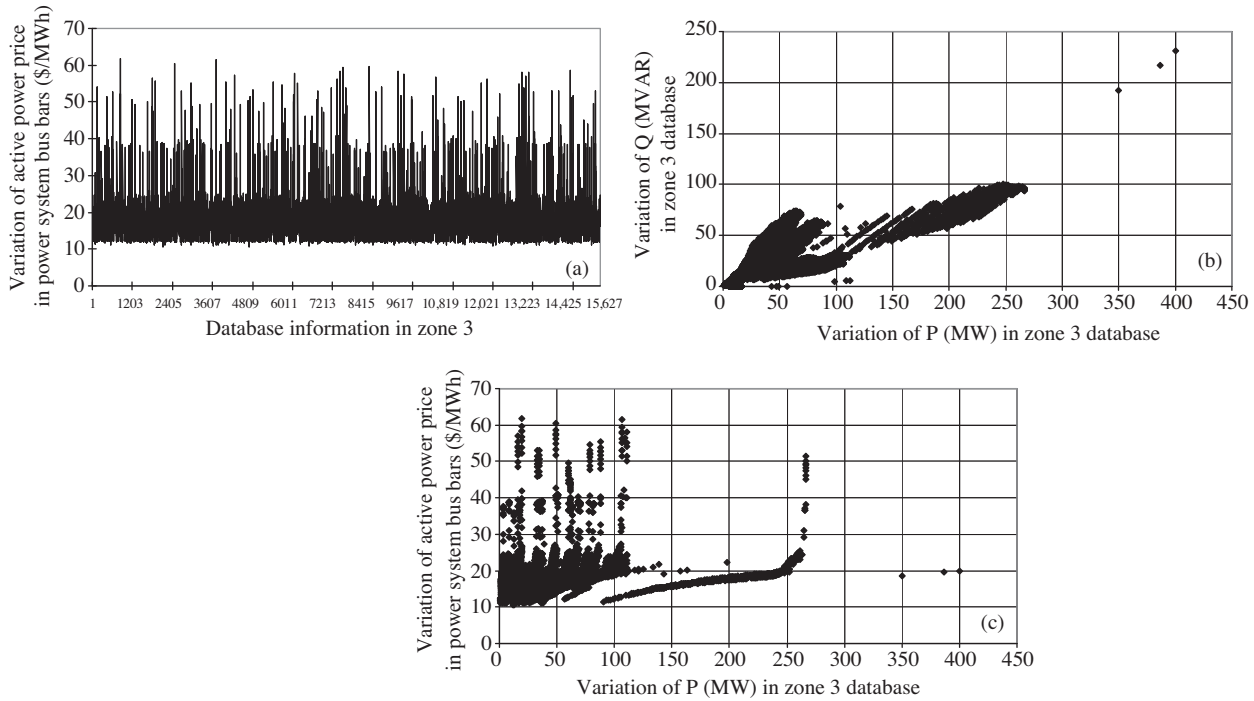
Figure 4. Zone 2 ANN database information: a) variation of 1 MWh of energy in terms of $/MWh b) active and reactive powers of load variations, c) active power price variations in terms of $/MWh on the basis of active power variations.

Figure 5. Zone 3 ANN database information: a) price variation of 1 MWh of energy in terms of $/MWh, b) active and reactive load power variations, c) variation of active power price in terms of $/MWh on the basis of active power variations.
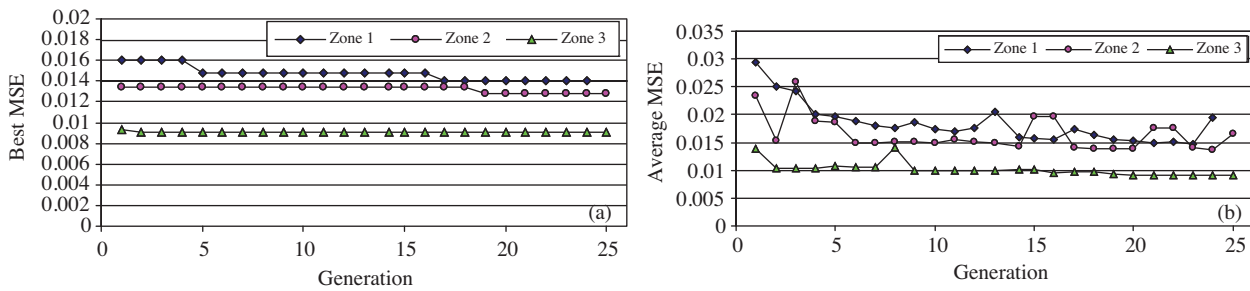
Figure 6. MSE fitness versus generation in all zones of ANN training: a) the best values, b) the average values.

In Figure 7, the sensitivity of the ANN to active and reactive power in all zones under testing conditions is presented. In Table 5, the minimum and maximum price sensitivities, rather than active and reactive power variations in all zones, are provided. It can be observed in Figure 7 that regarding the obtained ANN training, the price sensitivity to P and Q in zone 1 is larger than the sensitivity of other zones. Price variations based on active and reactive power in all zones during testing conditions are presented in Figures 8 and 9, respectively. It can be seen that zone 2 is more congested than the other zones. Furthermore, Figures 8 and 9 show that, due to congestion increase in zone 2, price variation in this zone (based on Figure 4a) is greater than in other zones.

Table 5. Maximum price sensitivity to active and reactive power variations in all zones.

Zone No.	Sensitivity	Price
Zone 1	P	0.439895693
	Q	0.229954278
Zone 2	P	0.075942479
	Q	0.094324891
Zone 3	P	0.049030118
	Q	0.059722095
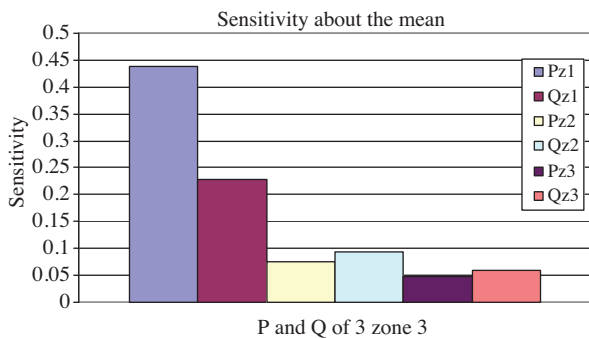
Figure 7. ANN sensitivity based on input parameters during testing conditions for all zones.
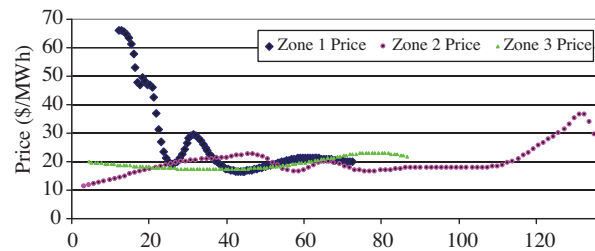
Figure 8. Price variation values in terms of active power (MW) variation in all zones during testing conditions.

For testing the accuracy of the proposed method, hour 19 was tested in all zones. That hour is near the peak load hour at which price spikes are most likely to occur. The price for all of the load nodes in the 3 zones of the power system on days 10, 19, and 25, which were considered for ANN testing, was forecasted. As an example, the amounts for day 19 are shown in Table 6.

Table 6. Price forecasting of all power system zones for 1900 hours on day 19. All active and reactive power values are in terms of MW and MVAR, respectively. All actual and forecasted prices are in terms of $/MWh.

Day 19 at 1900 hours, zone 1

Bus No.	P	Q	Actual price	ANN	ARIMA	GARCH
1	76.78	57.82	24.596	24.06	23.06	23.79
2	30.1	19.27	24.134	23.85	23.1	23.52
3	58.72	21.42	24.255	23.45	23.79	23.03
4	58.72	25.7	23.348	23.81	24.88	23.95
6	78.28	47.12	23.688	23.15	24.35	23.05
7	28.6	4.29	23.701	23.598	22.67	23.378
8	42.16	0	23.227	22.947	23.9	23.6
11	105.38	49.27	23.755	23.45	23.14	24.12
12	70.76	21.42	23.616	22.95	24.45	23.44
13	51.19	34.26	24.237	23.82	23.14	23.62
14	21.07	2.14	23.858	23.61	24.46	23.37
15	135.49	64.25	23.976	23.99	23.32	23.71
16	37.64	21.42	23.718	24.06	23.03	23.97
17	16.56	6.43	23.16	23.73	22.58	23.96
18	90.32	72.83	23.521	22.93	22.11	24.12
19	67.75	53.53	23.928	23.10	22.58	23.22
20	27.09	6.43	24.035	23.42	23.75	23.3
21	21.07	17.13	23.829	23.59	23.77	23.52
22	15.05	10.7	23.353	24.19	22.93	23.47
23	10.54	6.43	22.418	21.98	23.4	23.44
24	19.57	0	22.656	22.67	22.93	23.35
7	106.88	27.85	23.326	24.15	23.18	23.41
28	25.59	14.99	23.699	22.34	22.11	23.19
29	36.12	8.57	23.893	23.51	22.78	23.4
31	64.74	57.82	23.807	23.21	24.47	23.32
32	88.82	49.27	23.222	22.94	23.65	23.68
70	99.36	42.83	23.042	22.67	23.92	23.75
72	18.06	0	22.933	22.23	23.7	23.36
73	9.03	0	23.053	23.56	22.25	23.68
74	102.37	57.82	23.89	23.25	23.13	23.32
75	70.76	23.56	23.487	23.15	24.79	23.95
113	9.03	0	22.847	23.56	23.74	23.66
114	12.04	6.43	23.409	23.64	22.61	23.82
115	33.11	14.99	23.429	23.08	24.11	23.91
117	30.1	17.13	24.073	24.08	23.47	23.5

Day 19 at 1900 hours, zone 2

Bus No.	P	Q	Actual price	ANN	ARIMA	GARCH
33	34.62	19.27	24.148	23.60	23.24	24.73
34	88.82	55.68	23.716	23.46	24.78	24.01
35	49.69	19.27	23.68	23.81	23.11	23.98
36	46.68	36.4	23.641	21.68	20.44	25.17
39	40.65	23.56	25.075	24.21	23.81	23.1
40	99.36	49.27	25.526	23.67	23.11	23.43
41	55.71	21.42	25.757	25.99	24.93	25.11
42	144.53	49.27	25.28	24.18	26.12	24.32
43	27.09	14.99	24.306	24.84	23.63	24.99
44	24.08	17.13	24.282	24.59	23.82	23.21
45	79.79	47.1	23.974	22.84	22.68	22.79
46	42.16	21.42	22.772	21.86	23.65	23.82
47	51.19	0	22.702	21.86	21.43	21.67
48	30.1	23.56	22.663	21.59	23.77	21.5
49	130.96	64.25	22.408	22.53	23.11	22.76
50	25.59	8.57	22.734	20.39	24.47	20.45
51	25.59	17.13	23.139	22.82	22.42	22.01
52	27.09	10.7	23.314	22.49	22.01	22.34
53	34.62	23.56	23.104	21.58	21.33	21.62
54	170.11	68.54	22.553	22.91	23.33	23.07
55	94.84	47.12	22.574	22.37	21.98	22.91
56	126.46	38.55	22.603	23.18	23.66	23.31
57	18.06	6.43	22.81	20.03	19.89	20.11
58	18.06	6.43	23.023	22.03	21.69	21.87
59	417.02	242	22.425	22.71	23.01	22.89
60	117.43	6.43	22.117	21.38	21.12	21.31
62	115.93	29.99	22.015	21.05	20.74	20.82
66	58.72	38.55	21.615	22.46	22.94	22.7
67	42.16	14.99	21.996	20.05	19.92	20.13
76	102.37	77.09	23.135	24.19	24.72	24.65
77	91.83	59.96	22.066	22.01	23.25	22.91
78	106.88	55.68	22.207	22.41	22.76	23.11
79	58.72	68.54	22.144	23.08	23.57	23.29
80	195.72	55.68	21.578	22.39	22.41	22.87
97	22.58	19.27	21.497	20.71	22.67	20.45
98	51.19	17.13	21.12	22.36	22.94	22.45
99	63.23	0	19.065	20.93	21.14	22.76
116	277.01	0	21.982	23.36	23.78	24.43
118	49.67	32.12	23.558	22.57	22.23	22.02

Day 19 at 1900 hours, zone 3

Bus No.	P	Q	Actual price	ANN	ARIMA	GARCH
82	81.29	57.82	21.178	20.77	20.23	20.2
83	30.1	21.42	20.888	19.82	19.01	22.14
84	16.56	14.99	20.079	19.19	22.12	21.5
85	36.12	32.12	19.429	18.14	21.54	21
86	31.61	21.42	15.963	16.76	19.78	19.85
88	72.26	21.42	19.697	20.06	18.73	21.23
90	245.39	89.96	20.617	19.28	21.87	21.63
91	15.05	0	20.123	18.60	22.41	18.48
92	97.85	21.42	19.439	20.59	20.98	20.72
93	18.06	14.99	20.041	19.09	21.56	21.45
94	45.15	34.26	20.423	19.02	21.79	19.29
95	63.22	66.39	20.991	21.47	22.11	21.9
96	57.21	32.12	21.244	20.71	20.24	20.21
100	55.71	38.55	19.548	20.67	21.42	20.92
101	33.11	32.12	19.714	18.12	17.75	18.42
102	7.53	6.43	19.552	17.87	17.22	17.45
103	34.62	34.26	19.809	18.31	18.22	18.27
104	57.21	53.53	19.882	20.03	21.87	20.42
105	46.68	55.68	20.062	19.89	19.93	19.88
106	64.74	34.26	20.384	22.36	23.14	22.92
107	75.26	25.7	20.949	22.68	23.56	23.45
108	3.01	2.45	20.041	18.49	18.23	18.36
109	12.04	6.43	20.02	19.65	19.22	19.47
110	58.72	64.25	19.837	21.52	22.36	22.23
112	102.37	27.85	19.997	21.56	22.98	21.91

Figure 9. Price variation values in terms of reactive power (MVAR) variation in all zones during testing conditions.

The MSE, RMSE, MAE, and minimum and maximum of absolute error values for ANN response during testing conditions in all zones are presented in Table 7. These amounts were obtained with Eqs. (12), (13), and (14). These results show that the performance of the proposed method for price forecasting is very good. According to Table 7, the maximum absolute error for the proposed method is equal to \$2.87/MWh in zone 2 at 1900 hours on day 19. The minimum absolute error for all zones is considerable.

Table 7. Criteria of analysis of ANN response in testing conditions for all zones.

Performance Index	Zone 1			Zone 2			Zone 3		
	Day 10, 1900 hours	Day 19, 1900 hours	Day 25, 1900 hours	Day 10, 1900 hours	Day 19, 1900 hours	Day 25, 1900 hours	Day 10, 1900 hours	Day 19, 1900 hours	Day 25, 1900 hours
MSE (ANN)	0.4733	0.0763	0.3948	0.3093	0.4127	0.2899	0.1843	0.2886	0.2255
MSE (ARIMA)	0.7211	0.1512	1.142	1.9874	2.013	1.4532	2.653	4.635	1.8842
MSE (GARCH)	0.5423	0.098	0.9873	1.654	1.972	1.4121	1.154	3.4383	1.5724
RMSE (ANN)	0.688	0.2762	0.6283	0.5562	0.6424	0.5384	0.4294	0.5372	0.4749
RMSE (ARIMA)	0.8491	0.3889	1.068	1.4097	1.4187	1.2054	1.6288	2.1531	1.3726
RMSE (GARCH)	0.7364	0.3139	0.9936	1.2860	1.4042	1.1883	1.074	1.8542	1.2539
MAE (ANN)	1.0228	0.4696	1.1428	0.8202	0.9203	0.7391	0.9412	1.0913	0.8525
MAE (ARIMA)	1.7423	0.5072	2.1167	1.543	1.011	1.7621	2.0238	1.1714	2.2139
MAE (GARCH)	1.3451	0.3137	1.8942	1.3450	1.003	1.5011	1.8046	1.0098	2.01185
Min Abs Error (ANN)	0.065	0.007	0.074	0.043	0.056	0.064	0.125	0.148	0.023
Min Abs Error (ARIMA)	0.103	0.059	0.216	0.267	0.462	0.023	0.231	0.132	0.156
Min Abs Error (GARCH)	0.126	0.084	0.119	0.230	0.294	0.101	0.189	0.182	0.225
Max Abs Error (ANN)	2.498	1.359	2.461	1.923	2.78	2.473	1.64	1.976	1.941
Max Abs Error (ARIMA)	3.21	1.589	2.55	2.32	3.201	2.412	2.03	4.7645	2.54
Max Abs Error (GARCH)	2.98	1.225	2.49	1.961	3.695	2.523	1.79	4.094	2.12

For comparing the performance of the proposed method, the ARIMA and GARCH time series were considered. The simulation results of these methods are shown in Table 6 for 1900 hours on day 19. These results show that the proposed method has a better performance than the other times series for short-term nodal price forecasting. As shown in Table 7, except for the case of zone 3 on day 19 at 1900 hours, in all other cases, the MAE of the proposed method is less than that of the ARIMA and GARCH models. The MSE, RMSE, and maximum and minimum values of the absolute amounts of the proposed method are also better in

all cases than those of the other time series models. In most cases, the GARCH model had a better performance than the ARIMA time series. The curves in Figures 10a-10c show the actual and forecasted price variations for all forecasting methods of Table 6.
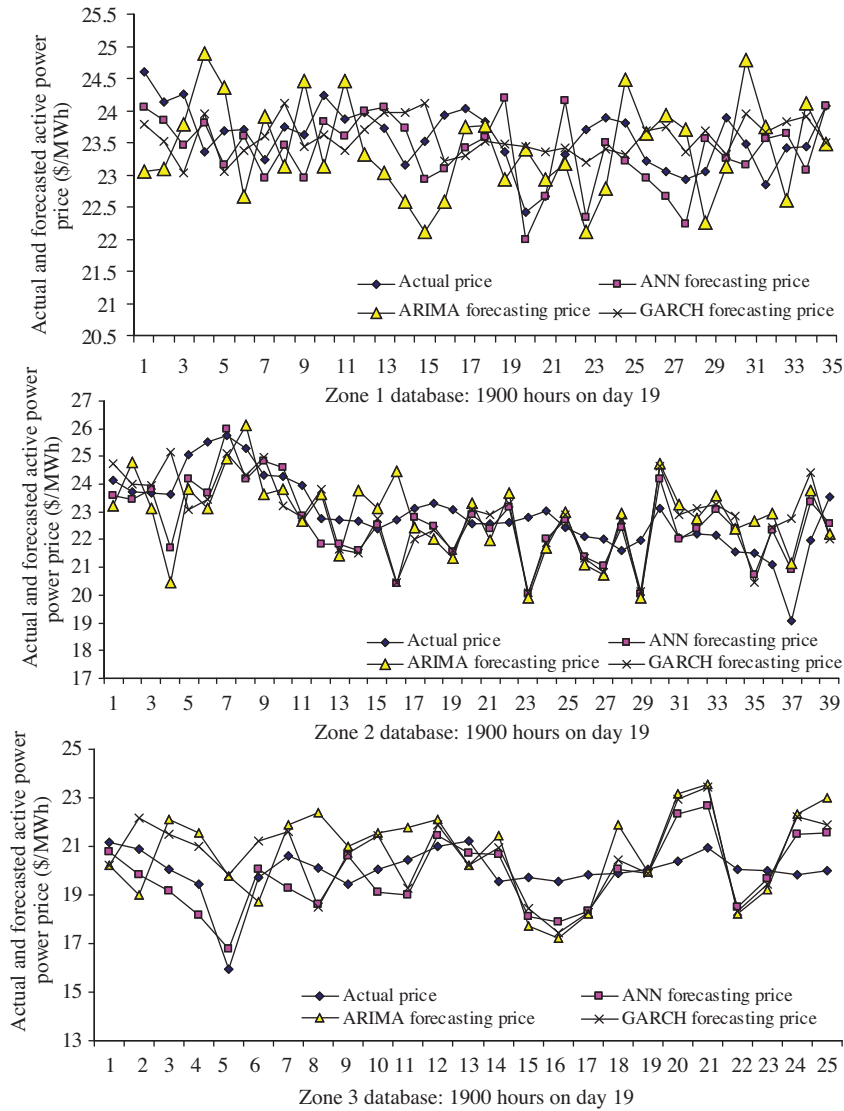
Figure 10. Actual and forecasted price variation for 1900 hours on day 19 in all power system zones: a) zone 1, b) zone 2, c) zone 3.

In real power markets, loading uncertainty, transmission constraints, and other factors lead to volatility for NCPs. Therefore, in spot markets, reliable and secure price forecast information help both transmission companies to schedule short-term generator outages and consumers to derive a plan to maximize their own utility with electricity purchased from the power market.

The test results obtained through the simulation demonstrate that the proposed algorithm is robust, efficient, and accurate. It produces better results than the ARIMA and GARCH time series for short-term nodal price forecasting. From the congestion management point of view, congestion management using this

nodal price is appropriate for maintaining network security. NCPs show the presence and the severity of congestion at different nodes in the power market. They provide an important signal to both power market participants and the ISO to handle the congestion problem.

The amounts shown in Table 6 demonstrate the ability of the proposed method for NCP forecasting with lower and more acceptable errors than the other time series methods in a short time span of only 9 s.

6.   Conclusions

In this paper, a new method for short-term NCP forecasting in a large-scale power market employing an ANN optimized by GA was proposed. The IEEE 118-bus test system was used for the proposed method's authenticity testing. To obtain the required database for training the neural network, all hours of a 30-day period were selected. The optimal power flow equations were then solved with regards to all of the effective constraints to determine the real price for each node. Finally, by dividing the network into 3 zones of forecasting and using a neural network for each zone, the price was determined. The comparison of the proposed method to the ARIMA and GARCH time series models shows the appropriate function of the proposed method for NCP forecasting and reduction of error, especially at locations of price spikes. The simulation results show that the proposed algorithm is robust, efficient, and accurate. It produces better results than the ARIMA and GARCH time series for short-term nodal price forecasting. In this method, NCPs directly indicate the presence and the severity of congestion at different nodes in the power system. It should be noted that the method produces an appropriate signal for both power market participants and the ISO to handle congestion problems and maintain network security.

Symbols

I	Set of the indices of generating units
J	Set of the indices of loads
Ji	Number of the load busbars in every zone
B	Set of system busbar indices
N	Set of transmission line indices
f_i	Generation cost of unit i, S/MWh
$P_{Gi\circ}$	Must-run active power generation of unit i
P_k, Q_k	Active and reactive injected powers in $k \in B$, MW, MVAR
$P_{L\circ j}, Q_{L\circ j}$	Uninterruptable active and reactive powers of load j
P_{gi}, Q_{gi}	Active and reactive power outputs of unit i, MW, MVAR
P_{Dj}, Q_{Dj}	Active and reactive powers of load j, MW, MVAR
$P_{g\min i}, P_{g\max i}$	Lower and upper limits of active power at unit i, MW
$Q_{g\min i}, Q_{g\max i}$	Lower and upper limits of reactive power at unit i, MVAR
$P_{D\min j}, P_{D\max j}$	Lower and upper limits of active power at load j, MW
$V_{\min k}, V_{\max k}$	Lower and upper limits of voltage magnitude at node k, p.u.
$R_{r\ AGC}(g_i)$	Ramp rate of unit i active power for load following/AGC, MW/min
$R_rQ(g_i)$	Ramp rate of unit i reactive power, MVAR/min
θ	Bus voltage angles, p.u.
I_{mk}	Line currents between nodes m and k, p.u.
P_{mk}	Real power flow between nodes m and k
$I_{mk\ \max}$	Upper limit of line current between nodes m and k
$P_{mk\ \max}$	Upper limit of real power flow through the line between nodes m and k
Rgi	Spinning reserve amount of unit i, MW

$Rgi_{\min}, Rgi_{\max}$ Lower and upper limits of spinning reserve of unit i, MW

P_{Aj}, P_{Fj} Actual and forecasted prices at node j, US\$/MWh

References

[1] N. Amjady, "Day-ahead price forecasting of electricity market by a new fuzzy neural network", IEEE Transactions on Power Systems, Vol. 21, pp. 888-896, 2006.

[2] S.K. Aggarwal, L.M. Saini, A. Kumar, "Electricity price forecasting in deregulated markets: a review and evaluation", Electrical Power and Energy Systems, Vol. 31, pp. 13-22, 2009.

[3] J. Contreras, R. Espinola, F.J. Nogales, A.J. Conejo, "ARIMA models to predict next-day electricity prices", IEEE Transactions on Power Systems, Vol. 18, pp. 1014-1020, 2003.

[4] A.J. Conejo, M.A. Plazas, R. Espinola, A.B. Molina, "Day-ahead electricity price forecasting using the wavelet transform and ARIMA models", IEEE Transactions on Power Systems, Vol. 20, pp. 1035-1042, 2005.

[5] M. Olsson, L. Söder, "Modeling real-time balancing power market prices using combined SARIMA and Markov processes", IEEE Transactions on Power Systems, Vol. 23, pp. 443-450, 2008.

[6] R.C. Garcia, J. Contreras, M. van Akkeren, J.B.C. Garcia, "A GARCH forecasting model to predict day-ahead electricity prices", IEEE Transactions on Power Systems, Vol. 20, pp. 867-874, 2005.

[7] H. Mori, A. Awata, "Normalized RBFN with hierarchical deterministic annealing clustering for electricity price forecasting", IEEE Power Engineering Society General Meeting, pp. 1-7, 2007.

[8] P. Areekul, T. Senjyu, H. Toyama A. Yona, "A hybrid ARIMA and neural network model for short-term price forecasting in deregulated market", IEEE Transactions on Power Systems, Vol. 25, pp. 524-530, 2010.

[9] A.T. Lora, J.R. Santos, J.C.R. Santos, A.G. Expósito, J.L.M. Ramos, "A comparison of two techniques for next-day electricity price forecasting", Proceedings of IDEAL, pp. 384-390, 2002.

[10] V. Nanduri, T.K. Das, "A reinforcement learning model to assess market power under auction-based energy pricing", IEEE Transactions on Power Systems, Vol. 22, pp 85-95, 2007.

[11] J.J. Guo, P.B. Luh, "Improving market clearing price prediction by using a committee machine of neural networks", IEEE Transactions on Power Systems, Vol. 19, pp. 1867-1876, 2004.

[12] P. Mandal, A.K. Srivastava, J.W. Park, "An effort to optimize similar days parameters for ANN-based electricity price forecasting", IEEE Transactions on Power Systems, Vol. 45, pp. 1888-1896, 2009.

[13] S.N. Pandey, S. Tapaswi, L. Srivastava, "Nodal congestion price estimation in spot power market using artificial neural network", IET Generation, Transmission & Distribution, Vol. 2, pp. 280-290, 2008.

[14] A. Wang, B. Ramsay, "Prediction of system marginal price in the UK power pool using neural network", International Conference on Neural Networks, Vol. 4, pp. 2116-2120, 1997.

[15] L. Zhang, P.B. Luh, "Neural network-based market clearing price prediction and confidence interval estimation with an improved extended Kalman filter method", IEEE Transactions on Power Systems, Vol. 20, pp. 59-66, 2005.

[16] B. Zhang, C. Zeng, S. Wang, "Forecasting market-clearing price in day-ahead market using SOM-ANN", Proceedings of 39th International Universities Power Engineering Conference, Vol. 1, pp. 390-393, 2004.

[17] G. Li, C.C. Liu, C. Mattson, J. Lawarrée, "Day-ahead electricity price forecasting in a grid environment", IEEE Transactions on Power Systems, Vol. 22, pp 266-274, 2007.

[18] N. Bigdeli, K. Afshar, N. Amjady, "Market data analysis and short-term price forecasting in the Iran electricity market with pay-as-bid payment mechanism", Electric Power Systems Research, Vol. 79, pp. 888-898, 2009.

[19] C.P. Rodriguez, G.J. Anders, "Energy price forecasting in the Ontario competitive power system market", IEEE Transactions on Power Systems, Vol. 19, pp. 366-374, 2004.

[20] B.J. Chen, M.W. Chang, C.J. Lin, "Load forecasting using support vector machines: a study on EUNITE competition 2001", IEEE Transactions on Power Systems, Vol. 19, pp. 1821-1830, 2004.

[21] J.K. Lee, J.B. Park, J.R. Shin, "A system marginal price forecasting based on an artificial neural network adapted with rough set theory", IEEE Power Engineering Society General Meeting, Vol. 1, pp. 528-533, 2005.

[22] A.J. Conejo, J. Contreras, R. Espinola, M.A. Plazas, "Forecasting electricity prices for a day-ahead pool-based electric energy market", International Journal of Forecasting, Vol. 21, pp. 435-462, 2005.

[23] M. Shahidehpour, H. Yamin, Z. Li, Market Operations in Electric Power Systems: Forecasting, Scheduling, and Risk Management, New York, John Wiley & Sons, 2002.

[24] M.T. Hagan, M.B. Menhaj, "Training feed forward networks with the Marquardt algorithm", IEEE Transactions on Neural Networks, Vol. 5, pp. 989-993, 1994.

[25] http://motor.ece.iit.edu/data/118bus_abreu.xls.

[26] J. Wang, M. Shahidehpour, Z. Li, "Security-constrained unit commitment with volatile wind power generation", IEEE Transactions on Power Systems, Vol. 23, pp. 1319-1327, 2008.